ASIAN JOURNAL OF CIVIL ENGINEERING (BHRC) VOL. 14, NO. 6 (2013)
PAGES 881-898

SEPARATION GAP, A CRITICAL FACTOR IN EARTHQUAKE INDUCED POUNDING BETWEEN ADJACENT BUILDINGS

S. Naserkhaki[*a,b], M. El-Rich[a], F.N.A. Abdul Aziz[b] and H. Pourmohammad[c]
[a]Department of Civil and Environmental Engineering, Faculty of Engineering, University of Alberta, Edmonton, Canada.
[b]Department of Civil Engineering, Faculty of Engineering, Universiti Putra Malaysia, Serdang, Malaysia.
[c]Department of Civil Engineering, Faculty of Engineering, Islamic Azad University, Karaj Branch, Karaj, Iran.

Received: 20 November 2012; **Accepted:** 18 April 2013

ABSTRACT

In this paper it is attempted to study seismic responses of adjacent buildings subjected to earthquake induced pounding and to clarify pounding effects for various separation gaps. An analytical model of adjacent buildings resting on a half-space is provided whilst the buildings are connected by visco-elastic contact force model. Results show that with same separation gap, adjacent buildings with structure-soil-structure interaction (SSSI) are more likely to pound together than buildings with fixed-based (FB) condition. Also, building condition gets worse due to pounding because the seismic responses of buildings are unfavourably increased and the condition becomes more critical if the separation gap becomes narrower.

Keywords: Separation gap; building pounding; seismic response; fixed-based (FB) buildings; structure-soil-structure interaction (SSSI); earthquake excitation.

1. INTRODUCTION

Pounding which is impact of adjacent buildings when they vibrate out of phase and separation gap between them is less than minimum distance required for them to vibrate freely due to earthquake excitations has caused building damage during almost every earthquake. For instance, damages of buildings because of pounding during 1985 Mexico City and 1989 Loma Prieta earthquakes were reported by Rosenblueth and Meli [1] and

[*] E-mail address of the corresponding author: s.naserkhaki@ualberta.ca (S. Naserkhaki)

Kasai and Maison [2], respectively. Even in recent earthquakes, despite great improvements in building codes, there are many evidences of buildings damage due to pounding [3-7].

Building codes in earthquake prone areas typically assign preventive provisions to avoid pounding between adjacent buildings. Minimum required separation gap to prevent pounding has been identified by different criteria based on different building codes. International Building Code (IBC) [8], specifies that separation gap between adjacent buildings with same property line shall be equal or greater than the Square Root of the Sum of the Squares (SRSS) of adjacent buildings maximum inelastic displacements while the ratio of Absolute Sum (ABS) of maximum inelastic displacements of adjacent buildings has been assigned as the minimum required separation gap by Taiwan Building Code (TBC) [9]. Studies conducted by Lin and Weng [10] and Lin [11] depicted that the minimum separation gap calculated from ABS method was 1.6 times greater than the minimum separation gap calculated from SRSS. On the other hand, Iran National Building Code (INBC) [12], roughly accepts minimum separation gap equal to 1% of building height; so edge of each building should be adjusted at least 0.5% of buildings height from its property line.

Despite of these building code provisions risk of building pounding is still high because;

- Existing and old buildings may not meet new building code requirements
- Building codes do not consider out of phase responses of buildings
- Building codes do not consider larger displacements due soil effect

Penzien [13] conducted a study to predict the minimum separation gap to avoid pounding during strong earthquakes for linear and nonlinear buildings. He found that there were possibilities of exceedance of the relative displacement than the values specified in the codes (SRSS and ABS) which would result in higher probabilities of building pounding. Hao and Shen [14] also concluded that SRSS provided up to 20% of underestimation for relative displacements of two buildings for substantially out of phase buildings because SRSS did not consider the response phase difference rigorously. Moreover, numerical study by Lin and Weng [15] demonstrated that the period ratio of adjacent buildings was an important parameter that affected the pounding risk of adjacent buildings while it was not considered in SRSS method.

To account for out of phase responses of buildings in probabilistic based approaches, inclusion of cross correlation coefficient has been proposed by Garcia and Soong [16-17] and Jeng and Kasai [18]. However, these methods are yet imperfect due to lack of soil effect considerations. Seismic responses of adjacent buildings become more out of phase due to soil because; i. lag time between input earthquake excitation percepted by remotely located buildings [18], ii. Spatially varying earthquakes [19] and iii. Change in dynamic behaviour of buildings [20]. Another effect of soil is enlargement of displacements which could be greater than those estimated by building codes [20-21].

Moreover, aforementioned studies all discuss about minimum separation gap required to prevent building pounding, but they are incapable of estimating seismic responses of building if pounding occurs. As discussed before it is undeniable that many buildings will subject to building pounding in future earthquakes as like as many buildings that already experienced pounding in past earthquakes. Therefore, finding seismic responses of buildings due to earthquake induced pounding is of interest which can be performed via time history analysis.

Formulation of building vibration due to earthquake induced pounding has been developed previously [22-25]. The significant effect of building pounding was found amplifying seismic responses of building particularly building story shear leading to building damage. The separation gap found to be critical in these studies by increasing the pounding effect with reduction of separation gap. The most important conclusion of all studies in this area is that neglecting of pounding effects could result in unconservative building design if the pounding potential is high. Despite of all these worthy researches, effect of soil was not considered in the analyses which is not an ignorable deficiency.

The aim of this research is to numerically study building pounding problem and investigate seismic responses of buildings due to earthquake induced pounding for various separation gaps. Seismic responses of two adjacent buildings resting on the soil due to earthquake induced pounding is evaluated. The seismic responses of buildings due to various separation gaps are obtained for two foundation conditions, fixed-based (FB) and structure-soil-structure interaction (SSSI), and the results are discussed.

2. DEVELOPMENT OF ANALYTICAL MODEL

Analytical model comprises two sub-models: i. adjacent buildings resting on a half-space vibrating individually free, and ii. pounding forces. Eventually, analytical model of pounding of adjacent buildings resting on a half-space is obtained by combination of these two sub-models.

2.1. Analytical model of adjacent buildings resting on a half-space

The buildings are assumed as shear buildings with concentrated mass, viscous damper and linear spring at each story and the soil as semi-infinite homogenous half-space as shown in Figure 1(a). Figure 1(b) shows analytical model of adjacent buildings resting on a half-space. Connection between building and soil is through interaction forces with equal magnitudes but opposite directions for building and soil. These interaction forces come from inertia forces corresponding to masses of building and soil called inertial interaction [26-27]. Moreover, adjacent buildings are coupled together through the soil and response of each building affects the other since they are located in near proximity which is called structure-soil-structure interaction or SSSI effect [27-28]. Equation of motion of two adjacent buildings with SSSI effect vibrating due to earthquake acceleration of $\ddot{u}_g(t)$ is:

$$\boldsymbol{M}_{bsb}\ddot{\boldsymbol{U}}_{bsb} + \boldsymbol{C}_{bsb}\dot{\boldsymbol{U}}_{bsb} + \boldsymbol{K}_{bsb}\boldsymbol{U}_{bsb} = -\left(\boldsymbol{M}_{bsb}\nu_{bsb} + \nu_{fbsb}\right)\ddot{u}_g(t) \tag{1}$$

$\boldsymbol{M}_{bsb}$, $\boldsymbol{C}_{bsb}$ and $\boldsymbol{K}_{bsb}$ are mass, damping and stiffness matrices with dimension of (n+m) by (n+m), respectively and $\ddot{\boldsymbol{U}}_{bsb}$, $\dot{\boldsymbol{U}}_{bsb}$, $\boldsymbol{U}_{bsb}$, ν_{bsb} and ν_{fbsb} are acceleration, velocity, displacement and influence vector of building and influence vector of soil with dimension of (n+m), respectively.

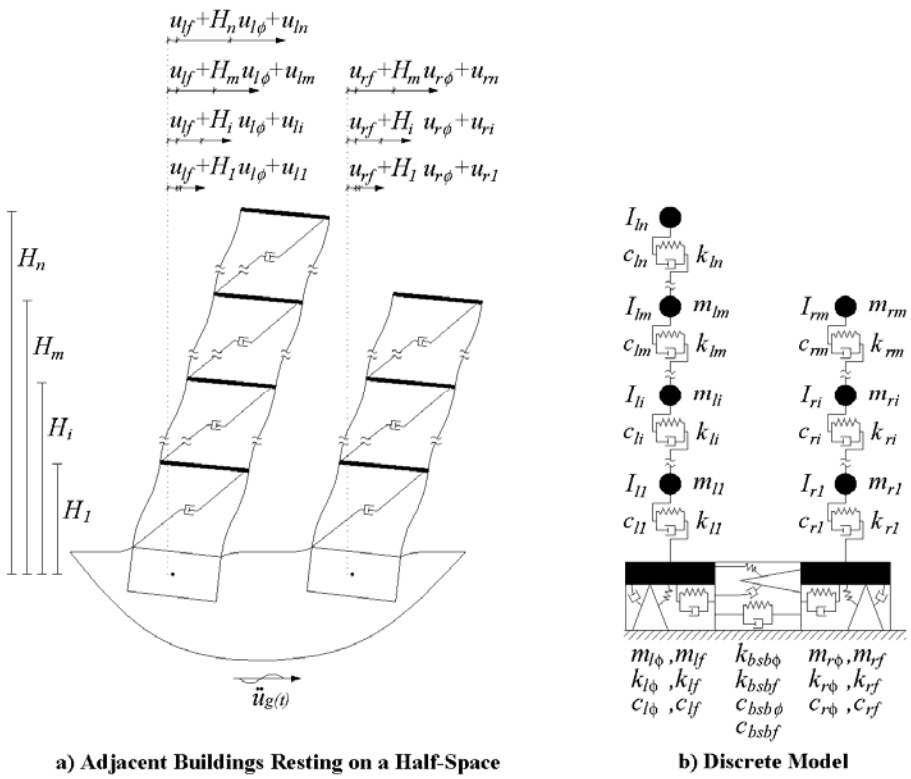

Figure 1. Analytical model of adjacent buildings resting on a half-space [20]

Equation (1) consists of two sets of equations corresponding to each building while two sets of equations are coupled together by off diagonal SSSI components of stiffness and damping matrices. The first set includes *n+2* coupled equations; *n* for NDOF left building and *2* for 2DOF soil. Similarly, the second set includes *m+2* coupled equations; *m* for MDOF right building and *2* for 2DOF soil ($n \geq m$). More sensible insight to Eq. (1) is presented by its expansion as:

$$\begin{bmatrix} \boldsymbol{m_{ls}} & \boldsymbol{m_{lbs}} & \boldsymbol{0} & \boldsymbol{0} \\ \boldsymbol{m_{lsb}} & \boldsymbol{m_{lb}} & \boldsymbol{0} & \boldsymbol{0} \\ \boldsymbol{0} & \boldsymbol{0} & \boldsymbol{m_{rs}} & \boldsymbol{m_{rbs}} \\ \boldsymbol{0} & \boldsymbol{0} & \boldsymbol{m_{rsb}} & \boldsymbol{m_{rb}} \end{bmatrix} \begin{Bmatrix} \ddot{\boldsymbol{u}}_{\boldsymbol{ls}} \\ \ddot{\boldsymbol{u}}_{\boldsymbol{lb}} \\ \ddot{\boldsymbol{u}}_{\boldsymbol{rs}} \\ \ddot{\boldsymbol{u}}_{\boldsymbol{rb}} \end{Bmatrix} + \begin{bmatrix} \boldsymbol{c_{ls}} & \boldsymbol{0} & \boldsymbol{c_{bsb}} & \boldsymbol{0} \\ \boldsymbol{0} & \boldsymbol{c_{lb}} & \boldsymbol{0} & \boldsymbol{0} \\ \boldsymbol{c_{bsb}} & \boldsymbol{0} & \boldsymbol{c_{rs}} & \boldsymbol{0} \\ \boldsymbol{0} & \boldsymbol{0} & \boldsymbol{0} & \boldsymbol{c_{rb}} \end{bmatrix} \begin{Bmatrix} \dot{\boldsymbol{u}}_{\boldsymbol{ls}} \\ \dot{\boldsymbol{u}}_{\boldsymbol{lb}} \\ \dot{\boldsymbol{u}}_{\boldsymbol{rs}} \\ \dot{\boldsymbol{u}}_{\boldsymbol{rb}} \end{Bmatrix}$$

$$+ \begin{bmatrix} \boldsymbol{k_{ls}} & \boldsymbol{0} & \boldsymbol{k_{bsb}} & \boldsymbol{0} \\ \boldsymbol{0} & \boldsymbol{k_{lb}} & \boldsymbol{0} & \boldsymbol{0} \\ \boldsymbol{k_{bsb}} & \boldsymbol{0} & \boldsymbol{k_{rs}} & \boldsymbol{0} \\ \boldsymbol{0} & \boldsymbol{0} & \boldsymbol{0} & \boldsymbol{k_{rb}} \end{bmatrix} \begin{Bmatrix} \boldsymbol{u_{ls}} \\ \boldsymbol{u_{lb}} \\ \boldsymbol{u_{rs}} \\ \boldsymbol{u_{rb}} \end{Bmatrix} = -\left(\begin{bmatrix} \boldsymbol{m_{ls}} & \boldsymbol{m_{lbs}} & \boldsymbol{0} & \boldsymbol{0} \\ \boldsymbol{m_{lsb}} & \boldsymbol{m_{lb}} & \boldsymbol{0} & \boldsymbol{0} \\ \boldsymbol{0} & \boldsymbol{0} & \boldsymbol{m_{rs}} & \boldsymbol{m_{rbs}} \\ \boldsymbol{0} & \boldsymbol{0} & \boldsymbol{m_{rsb}} & \boldsymbol{m_{rb}} \end{bmatrix} \begin{Bmatrix} \boldsymbol{0} \\ \boldsymbol{v_{lb}} \\ \boldsymbol{0} \\ \boldsymbol{v_{rb}} \end{Bmatrix} + \begin{Bmatrix} \boldsymbol{v_{ls}} \\ \boldsymbol{0} \\ \boldsymbol{v_{rs}} \\ \boldsymbol{0} \end{Bmatrix} \right) \ddot{u}_g \quad (2)$$

Definitions of variables of Eq. (1) is still valid for Eq. (2) while subscripts *l* and *r* stand for left and right buildings; *b* and *s* for building and soil; *bs* (*sb* is transpose of *bs*) and *bsb* for soil-structure interaction (SSI) and structure-soil-structure interaction (SSSI), respectively. Matrices and vectors of Eq. (2) are introduced in the following:

$\boldsymbol{m_{lb}}$ and $\boldsymbol{m_{rb}}$ are the mass matrices of the adjacent buildings which are generated from mass of each story which is concentrated at the floor level as shown in Figure 1(b). $\boldsymbol{k_{lb}}$ and $\boldsymbol{k_{rb}}$ are the stiffness matrices of the adjacent buildings which are generated from lateral stiffness of each story of the building as shown in Figure 1(b). $\boldsymbol{c_{lb}}$ and $\boldsymbol{c_{rb}}$ are the Rayleigh damping matrices of the adjacent building proportional to the mass and stiffness matrices.

$\boldsymbol{m_{ls}}$ and $\boldsymbol{m_{rs}}$ are matrices corresponding to the virtual mass of the soil beneath the adjacent buildings. $\boldsymbol{k_{ls}}$ and $\boldsymbol{k_{rs}}$ are matrices corresponding to the stiffness of the soil beneath the adjacent buildings. $\boldsymbol{c_{ls}}$ and $\boldsymbol{c_{rs}}$ are matrices corresponding to the damping of the soil beneath the adjacent buildings. Both rocking (denoted by ϕ) and horizontal (denoted by *f*) deformations of the soil are involved in these matrices providing the SSI effect. These matrices are generated from the coefficients defined in the time domain based on the basic constants of soil including shear modulus of soil (G), shear wave velocity of soil (V_s) and Poisson's ratio of soil (ν) and width of foundation (a) as shown in Figure 1(b) [27].

$\boldsymbol{k_{bsb}}$ and $\boldsymbol{c_{bsb}}$ are matrices corresponding to the stiffness and damping of the soil between two adjacent buildings, respectively. These matrices are providing the SSSI effect, so the adjacent buildings are coupled together through the soil. They are generated from the coefficients defined in the time domain based on the basic constants of soil as shown in Figure 1(b) [27].

Seismic responses of two adjacent buildings resting on a half-space subjected to earthquake acceleration is obtained from Eq. (2), however, pounding of buildings is not involved in this equation.

2.2. Analytical model of pounding

Pounding of two adjacent buildings can be simplified as pounding of different masses corresponding to each building at the same level. During the pounding, pounding force between adjacent pounded floors is modelled by a visco-elastic contact force model. It provides pounding force by a linear spring and dissipation of energy by a dashpot. Relationship between pounding force and displacement is shown in Figure 2. The only deficiency of linear visco-elastic contact model is providing tension forces at the end of pounding with no physical meaning which is ignorable [29].

Figure 3(a) demonstrates analytical model of buildings connected by linear visco-elastic contact force model. Contact force model is inactive when the buildings vibrate individually free, however, it is activated when the separation gap is closed and adjacent buildings pound together. Immediately upon the pounding, pounding force at *i*th floor is developed as:

$$F_{pi} = k_{sgi}\delta u_i + c_{sgi}\delta \dot{u}_i \tag{3}$$

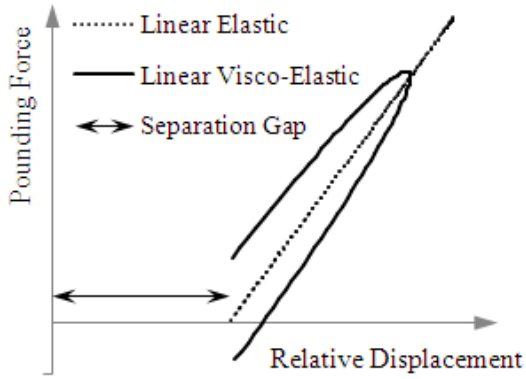

Figure 2. Pounding force and displacement relationship [24]

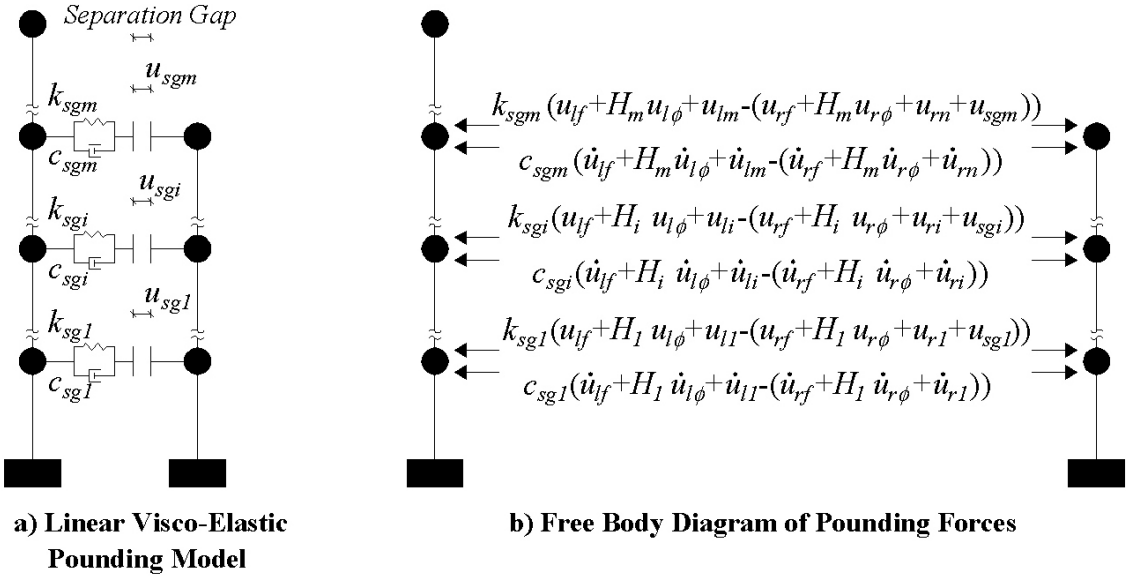

Figure 3. Analytical model of pounding [20]

δu_i is relative displacement and $\delta \dot{u}_i$ is relative velocity between *i*th adjacent floors. k_{sgi} and c_{sgi} are contact stiffness and damping coefficient of the *i*th floor, respectively. Contact stiffness, k_{sgi}, is taken as 10000 MN/m [20, 24-25]. Contact damping coefficient, c_{sgi}, depends on the pounded floor properties and coefficient of restitution which is taken as $e=0.65$ [20, 24-25].

The pounding force is developed during the pounding between the adjacent pounded floors only. Not necessarily all the floors pounded together at the same time. Free body diagram of pounding forces developed between all adjacent floors is shown in Figure 3(b). Pounding force is equal in both buildings but opposite direction. Assuming all the floors pounded together, equilibrium of pounding forces is then satisfied by:

$$\boldsymbol{C}_p\dot{\boldsymbol{U}}_{bsb} + \boldsymbol{K}_p\boldsymbol{U}_{bsb} = \boldsymbol{K}_p\boldsymbol{U}_{sg} \tag{4}$$

$\boldsymbol{C}_p$ and $\boldsymbol{K}_p$ are the damping and stiffness matrices of contact force model with dimension of (n+m) by (n+m), respectively, and $\boldsymbol{U}_{sg}$ is separation gap vector with dimension of (n+m). More sensible insight to Eq. (4) is presented by its expansion as:

$$\begin{bmatrix} \boldsymbol{c}_{p1} & \boldsymbol{c}_{p12} & 0 & -\boldsymbol{c}_{p1} & -\boldsymbol{c}_{p12} \\ & \boldsymbol{c}_{p2} & 0 & -\boldsymbol{c}_{p21} & -\boldsymbol{c}_{p2} \\ & & 0 & 0 & 0 \\ & \boldsymbol{SYM.} & & \boldsymbol{c}_{p1} & \boldsymbol{c}_{p12} \\ & & & & \boldsymbol{c}_{p2} \end{bmatrix} \begin{Bmatrix} \dot{\boldsymbol{u}}_{ls} \\ \dot{\boldsymbol{u}}_{lbm} \\ \dot{\boldsymbol{u}}_{lbn} \\ \dot{\boldsymbol{u}}_{rs} \\ \dot{\boldsymbol{u}}_{rb} \end{Bmatrix} + \begin{bmatrix} \boldsymbol{k}_{p1} & \boldsymbol{k}_{p12} & 0 & -\boldsymbol{k}_{p1} & -\boldsymbol{k}_{p12} \\ & \boldsymbol{k}_{p2} & 0 & -\boldsymbol{k}_{p21} & -\boldsymbol{k}_{p2} \\ & & 0 & 0 & 0 \\ & \boldsymbol{SYM.} & & \boldsymbol{k}_{p1} & \boldsymbol{k}_{p12} \\ & & & & \boldsymbol{k}_{p2} \end{bmatrix} \begin{Bmatrix} \boldsymbol{u}_{ls} \\ \boldsymbol{u}_{lbm} \\ \boldsymbol{u}_{lbn} \\ \boldsymbol{u}_{rs} \\ \boldsymbol{u}_{rb} \end{Bmatrix}$$

$$= \begin{bmatrix} \boldsymbol{k}_{p1} & \boldsymbol{k}_{p12} & 0 & -\boldsymbol{k}_{p1} & -\boldsymbol{k}_{p12} \\ & \boldsymbol{k}_{p2} & 0 & -\boldsymbol{k}_{p21} & -\boldsymbol{k}_{p2} \\ & & 0 & 0 & 0 \\ & \boldsymbol{SYM.} & & \boldsymbol{k}_{p1} & \boldsymbol{k}_{p12} \\ & & & & \boldsymbol{k}_{p2} \end{bmatrix} \begin{Bmatrix} \boldsymbol{0} \\ \boldsymbol{u}_{sgm} \\ \boldsymbol{0} \\ \boldsymbol{0} \\ \boldsymbol{0} \end{Bmatrix} \tag{5}$$

(Note: $\dot{\boldsymbol{u}}_{lb} = \dot{\boldsymbol{u}}_{lbm} + \dot{\boldsymbol{u}}_{lbn}$ and $\boldsymbol{u}_{lb} = \boldsymbol{u}_{lbm} + \boldsymbol{u}_{lbn}$)

Matrices and vector of contact force model are written as:

$$\boldsymbol{k}_{p1} = \begin{bmatrix} \sum_{i=1}^{m} H_i^2 k_{sgi} & \sum_{i=1}^{m} H_i\, k_{sgi} \\ \sum_{i=1}^{m} H_i\, k_{sgi} & \sum_{i=1}^{m} k_{sgi} \end{bmatrix} \tag{6}$$

$$\boldsymbol{k}_{p2} = \begin{bmatrix} k_{sg1} & \cdots & 0 \\ \vdots & \ddots & \vdots \\ 0 & \cdots & k_{sgm} \end{bmatrix} \tag{7}$$

$$\boldsymbol{k}_{p12} = \boldsymbol{k}_{p21}^{T} = \begin{bmatrix} H_1 k_{sg1} & \cdots & H_m k_{sgm} \\ k_{sg1} & \cdots & k_{sgm} \end{bmatrix} \tag{8}$$

$$\boldsymbol{u}_{sgm}^{T} = \{u_{sg1} \quad \cdots \quad u_{sgm}\} \tag{9}$$

$\boldsymbol{C}_p$ is derived as same as $\boldsymbol{K}_p$ except k_{sgi} is replaced by c_{sgi}. Matrices of contact force model ($\boldsymbol{C}_p$ and $\boldsymbol{K}_p$) derived above are for the case when all adjacent floor are pounded

together. Since different combination of pounding between adjacent floors occur during the earthquake, these matrices are altered accordingly. Those components of these matrices that correspond to the pounded floors take a non-zero value and the rest take zero value.

2.3. Analytical model of pounding of adjacent buildings resting on a half-space

Equations of motion of two adjacent buildings with SSSI effect (Eq. (1)) and equation of pounding forces (Eq. (4)) were provided separately in two previous sub-sections. By linear superposition of these two equations, equation of motion of pounding of two adjacent buildings considering SSSI effect is obtained as:

$$\boldsymbol{M}_{bsb}\ddot{\boldsymbol{U}}_{bsb} + \left(\boldsymbol{C}_{bsb} + \boldsymbol{C}_{p}\right)\dot{\boldsymbol{U}}_{bsb} + \left(\boldsymbol{K}_{bsb} + \boldsymbol{K}_{p}\right)\boldsymbol{U}_{bsb} = -\left(\boldsymbol{M}_{bsb}\nu_{bsb} + \nu_{fbsb}\right)\ddot{u}_{g}(t) + \boldsymbol{K}_{p}\boldsymbol{U}_{sg} \quad (10)$$

Before using Eq. (10), two states of the building responses must be diagnosed; no-pounding and pounding states. Boundary between these two states is defined by the following condition for *i*th floor:

no-pounding state: $$\left(u_{lf} + H_i u_{l\phi} + u_{li}\right) - \left(u_{rf} + H_i u_{r\phi} + u_{ri} + u_{sgi}\right) < 0 \quad (11a)$$

pounding state: $$\left(u_{lf} + H_i u_{l\phi} + u_{li}\right) - \left(u_{rf} + H_i u_{r\phi} + u_{ri} + u_{sgi}\right) \geq 0 \quad (11b)$$

When the buildings do not pound during earthquake excitation and the separation gap is open, no-pounding state condition is satisfied and therefore the pounding matrices ($\boldsymbol{C}_p$ and $\boldsymbol{K}_p$) in Eq. (10) are zero and the Eq. 10 reduces to Eq. (1). On the other hand, if the pounding state condition is satisfied during the earthquake excitation, the separation gap is closed and all terms and parameters of Eq. (10) are effective. Having Eq. (10), the adjacent buildings with both FB and SSSI conditions can be analyzed.

3. NUMERICAL STUDY

Obtaining seismic responses of buildings during earthquake excitation requires to solve a second order linear ordinary differential equation (Eq. (10)). This equation is, however, conceptually nonlinear since its characteristics are changed periodically from no-pounding to pounding state and vice versa during the analysis. This equation is solved employing Newmark method with linear acceleration response [30]. The equation and its solution were implemented using a computer program code. Time steps equal to 0.01 and 0.001 sec are taken for seismic analyses during no-pounding and pounding states, respectively. These time steps ensure accuracy and computational efficiency with minimum storage capacity of the output results.

Building configuration comprises a 7-story building in the left side which is adjacent to a 4-story building in the right side. The buildings are supposed to be residential buildings with mass of 100 Ton per story which gives fundamental periods of 0.784 and 0.451 sec for 7-story and 4-story buildings, respectively. These periods imply that 7-story building behaves relatively flexible while 4-story buildings relatively stiff. Acceleration record time history of

El Centro earthquake (I-ELC180 1940) is selected and applied to the building configurations.

Where SSSI condition is considered, soil is supposed to have shear wave velocity equal to 140 m/s, shear modulus equal to 32.34 MN/m^2 and Poisson's ratio equal to 0.35. The soil essentially causes elongation of building period where building period is increased about 12% for both buildings due to soil i.e. 0.878 and 0.505 sec 7-story and 4-story buildings, receptively.

3.1. Minimum required separation gap

Initially, minimum separation gap required to prevent pounding is calculated for the building configuration. Figure 4 shows variation of minimum required separation gap for different soil types (i.e. different shear wave velocities of soil). Minimum required separation gap is increased with reduction of soil shear wave velocity, or in another word, wider minimum separation gap is required to prevent pounding between adjacent buildings resting on softer soils. Fixed-based (FB) buildings do not pound if the separation gap is 0.096 m, however, for the structure-soil-structure interaction (SSSI) buildings about 46% wider separation gap (i.e. 0.140 m) is required to prevent pounding. Therefore, at the first stage it is concluded that wider separation gaps are required for the buildings resting on the soft soil. Besides, adjacent buildings resting on the soft soil (SSSI buildings) are in higher risk of pounding occurrence than the same buildings resting on hard soil (FB buildings).

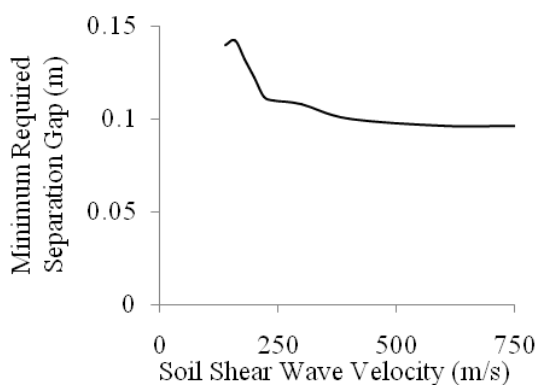

Figure 4. Minimum required separation gap versus different soil types

3.2. Seismic responses of buildings

Seismic responses of buildings due to the El Centro earthquake acceleration are obtained and envelopes of maximum seismic responses of buildings are presented in Figures 5 to 8. Seismic responses of buildings without pounding refer as N-FB and N-SSSI for fixed-based (FB) and structure-soil-structure interaction (SSSI) buildings, respectively, in these figures. For pounding cases, seismic responses are obtained considering separation gaps of 0.08 m (SG 0.08 m), 0.04 m (SG 0.04 m) and 0.00 m (SG 0.00 m).

Envelopes of maximum displacements of buildings are shown in Figures 5 and 6 for FB and SSSI buildings, respectively. 7-story building experiences smaller maximum displacements after pounding while displacement reduction is justified through all floor

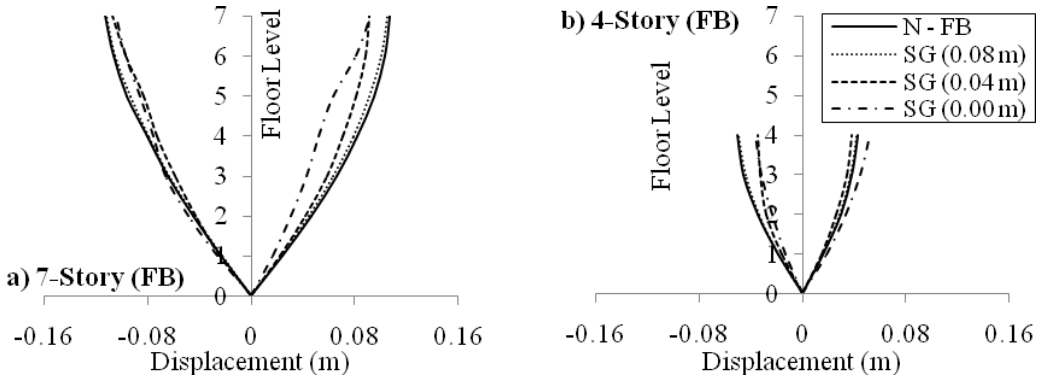

Figure 5. Envelopes of maximum displacements of buildings (FB)

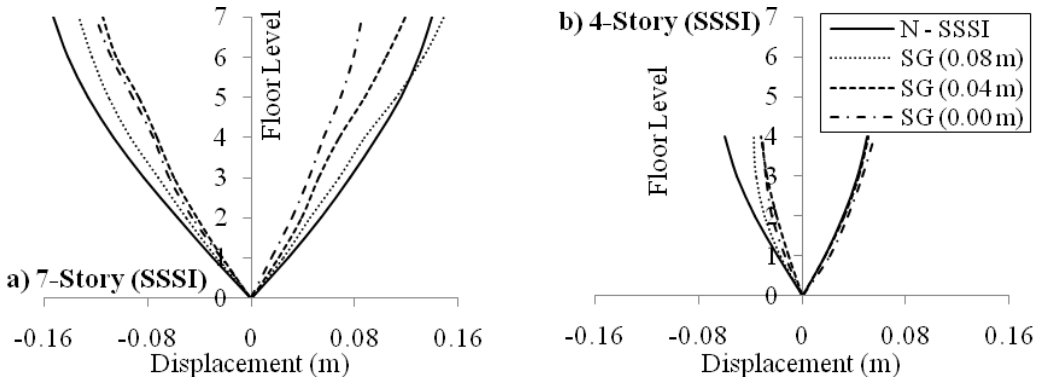

Figure 6. Envelopes of maximum displacements of buildings (SSSI)

levels of both sides. Although both FB (Figure 5(a)) and SSSI (Figure 6(a)) buildings demonstrate a similar pattern, but larger displacements are obvious for SSSI building. This is because of additional displacement imposed to the building due to soil which is profound in upper levels owing to rocking component of soil.

Pattern of produced story shear is different from displacement of 7-story building after pounding. Story shears are decreased in through pounding floors while increased in above pounding floors as shown in Figure 7(a) and Figure 8(a). When the buildings pound together, through pounding floors of 7-story building are prevented to move further by adjacent building while above pounding floors move freely which causes a sudden jump between displacements of through pounding and above pounding floors in pounding side which is visible in Figures 5(a) and 6(a). While relative displacements are reduced in through pounding floors, this sudden jump causes increment of relative displacements in above pounding floors like whiplash behaviour. Consequently, sharp story shears are produced above the pounding floors as shown in Figures 7(a) and 9(a). Comparing produced story shears of FB (Figure 7(a)) and SSSI (Figure 8(a)) buildings reveals that while soil causes reduction of story shear for buildings without pounding, it causes amplification of story shear after pounding. Reduction of story shear is because of reduction of relative displacements due to rocking component of soil in buildings without pounding, while

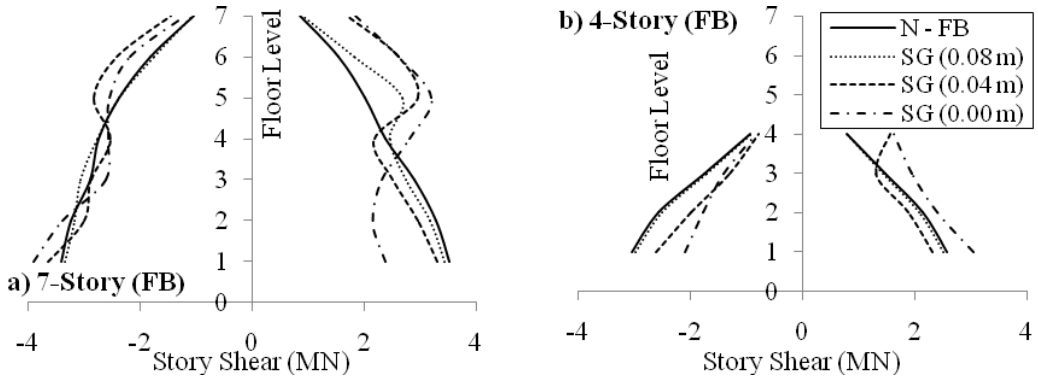

Figure 7. Envelopes of maximum story shears of buildings (FB)

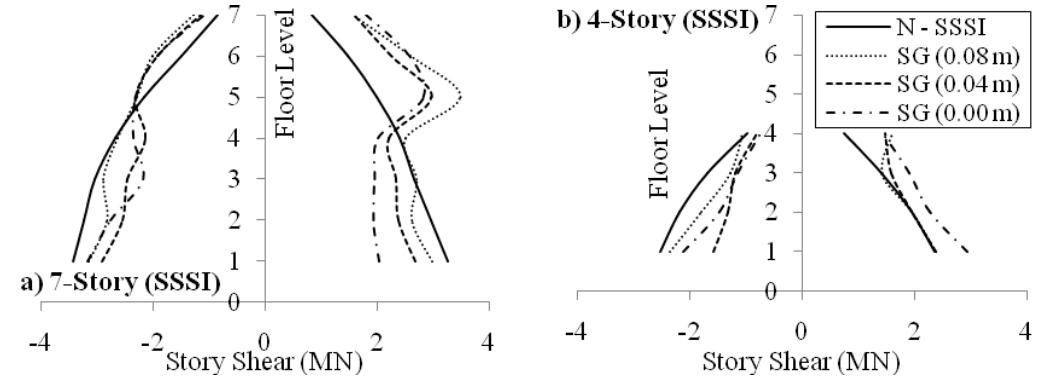

Figure 8. Envelopes of maximum story shears of buildings (SSSI)

pounding suppresses rocking effect of soil.

For 4-story building, both displacements and story shears of all floors are decreased in pounding side while increased in no-pounding side. 4-story building is prevented to move in pounding side but is pushed by adjacent building away after pounding which not only produces larger displacements (Figure 5(b) and Figure 6(b)) but also larger relative displacements and consequently greater story shears (Figure 7(b) and Figure 8(b)) in its no-pounding side. For 4-story building the same result as 7-story building is found by comparing FB and SSSI buildings.

Comparing seismic responses of buildings depicts that effect of pounding is more remarkable for smaller separation gaps. If separation gap is relatively wide seismic responses of buildings are close to seismic responses of buildings without pounding (e.g. compare N-FB and SG (0.08 m) in Figure 5 and Figure 7). When the separation gap is virtually zero (SG (0.00 m)) the buildings are affected by complete pounding and seismic responses experience the maximum deviation from no-pounding case (e.g. compare N-FB and SG (0.00 m) in Figures 5 and 7).

More sensible insight of influence of separation gap is given by observing first 15 sec history of seismic responses of buildings as shown in Figures 9 and 10. Displacement time history of 4th floor of buildings and corresponding pounding force time histories are

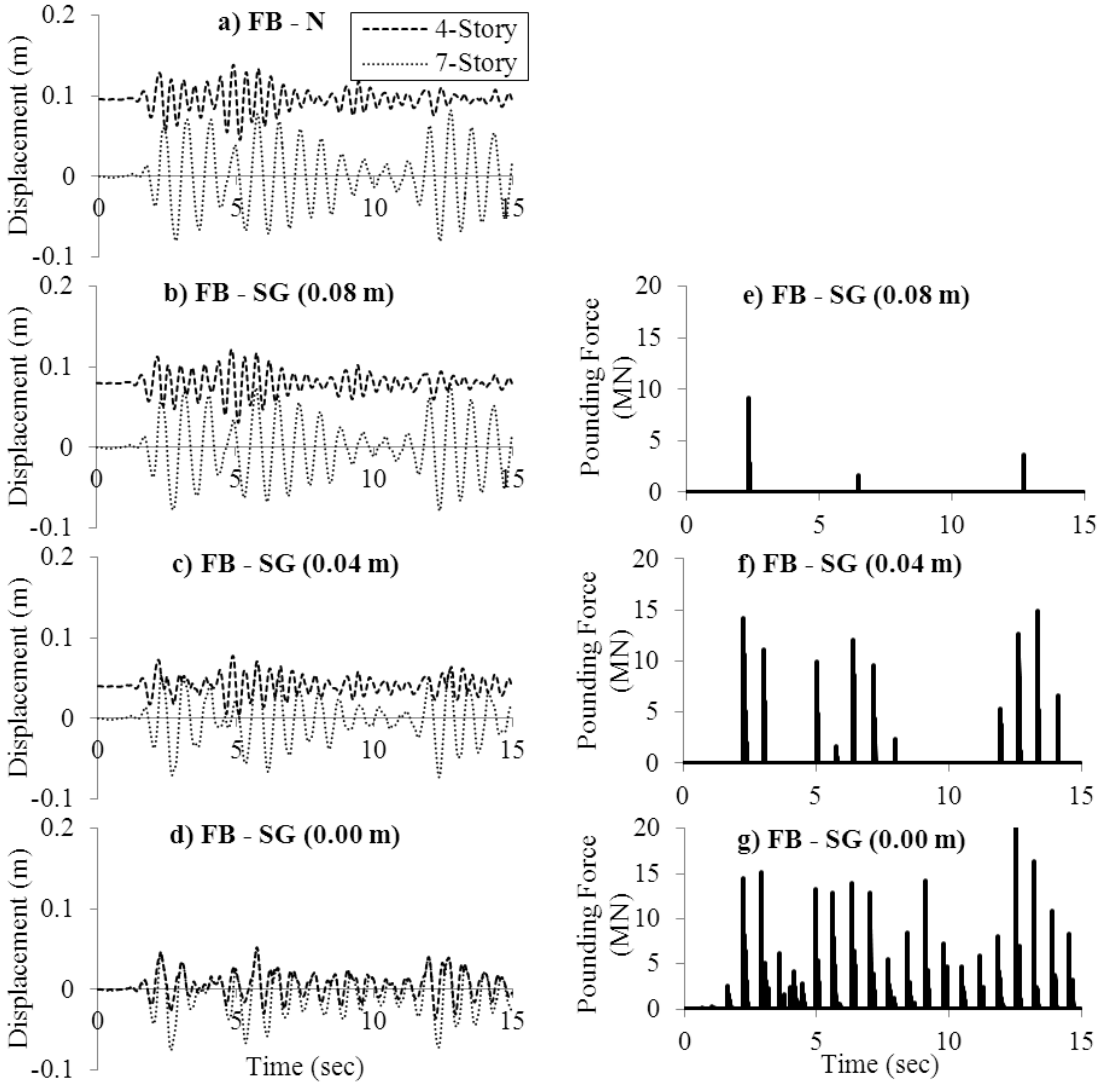

Figure 9. Time history of displacement and pounding forces produced at 4th floor of buildings (FB)

presented in Figures 9 and 10 for FB and SSSI buildings, respectively. Figure 9(a) shows time history of 4th floor of FB buildings; separation gap is 0.96 m and the buildings vibrate individually free and without pounding while the potential time of pounding is 2.5 sec. First building pounding occurs at 2.34 sec if separation gap is reduced to 0.08 m (Figure 9(b)). Change of seismic responses is slight compare to no-pounding case and the maximum response occurs at the same time as no-pounding case. Associated with each pounding is pounding force as shown in Figure 9(e) for separation gap of 0.08 m. Reducing separation gap to 0.04 m, more poundings occur between the buildings and greater pounding forces are developed as shown in Figure 9(c) and Figure 9(f). When the separation gap is virtually zero (SG (0.00 m)), buildings are pounded almost from beginning of the vibration at 0.03 sec

which is followed by several other poundings during the building vibration (Figure 9(d) and Figure 9(g)). At this separation gap very intense pounding occurs with large pounding forces developed between the buildings and vibration of either building is totally affected by the other and both buildings accompany each other during the vibration. Moreover, seismic responses are significantly altered; time of occurrence of the maximum displacement is different from no-pounding case since pounding alters displacement phase.

Comparing displacement time history of FB and SSSI buildings reveals that soil not only alters amplitude of the response but also changes its phase. While minimum separation gap to prevent pounding is 0.96 m and the potential time of pounding is 2.5 sec for FB building

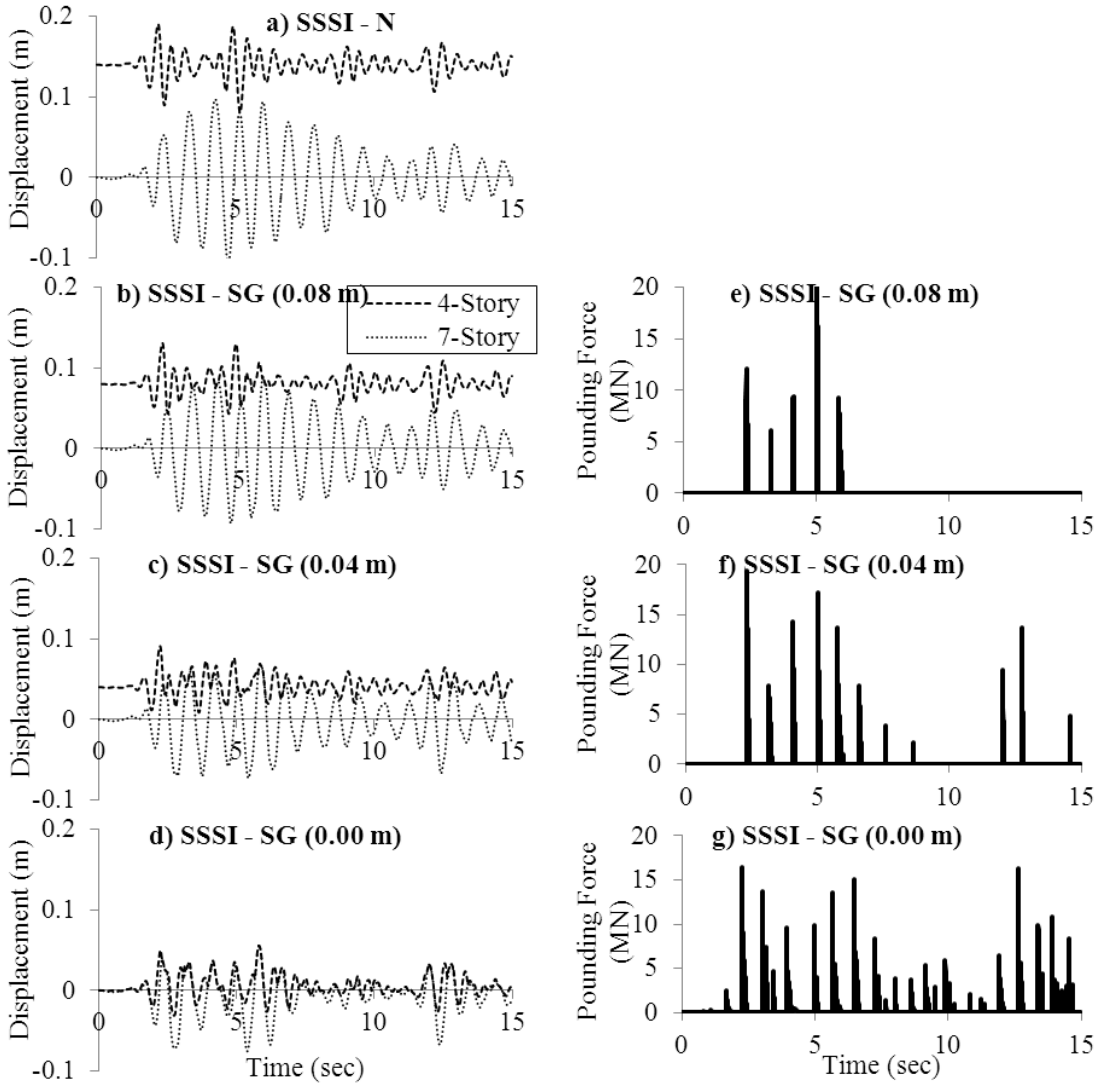

Figure 10. Time history of displacement and pounding forces produced at 4th floor of buildings (SSSI)

(Figure 9(a)), they are 0.140 m and 5.2 sec, respectively, for SSSI building (Figure 10(a)). Although separation gap of 0.08 m is relatively wide for FB building (Figure 9(b) and Figure 9(e)) but it provides a relatively narrow separation gap for SSSI building with more pounding occurrences during the vibration (Figure 10(b) and Figure 10(e)) and same trends go for smaller separation gaps.

In a nut shell, effect of pounding is different for each building, building side and floor level, anyhow, consequences of pounding is generally detrimental for both buildings since seismic responses of buildings, particularly story shear of buildings, are amplified due to pounding. The critical condition occurs at top floor of either building where story shears are increased dramatically. It is also found that soil alters building seismic responses and building may experience greater seismic responses considering soft soil. Finally, effect of pounding is more remarkable for smaller separation gaps where number of pounding occurrences and intensity of pounding are increased by reduction of separation gap.

3.3. Effect of separation gap

Variations of maximum pounding forces developed at the pounded floors are shown in Figure 11 with respect to separation gap. The minimum required separation gap is 0.096 and 0.140 m for FB and SSSI buildings, respectively, so no pounding force is observed beyond these separation gaps. Adjacent buildings pound together and pounding forces are developed when separation gap is less than these minimum values.

The minimum separation gap is greater for SSSI than FB buildings, because displacement of SSSI buildings are affected by rocking component of soil. When the separation gap is between 0.096 and 0.140 m, only 4th floor of adjacent buildings with SSSI condition pound together. When the separation gap is reduced to below 0.096 m, 4th floor of adjacent buildings with FB condition pound together too. More reduction of the separation gap results in pounding between lower floors; 3rd, 2nd and 1st floors, respectively. It is observed in this figure, though the minimum separation gap required to prevent pounding is significantly greater for SSSI buildings than FB building at 4th floor, it is slightly greater for SSSI buildings than FB building at the 3rd floor. This trend is even reversed at 2nd and 1st floors where the minimum separation gap required to prevent pounding is less for SSSI buildings than FB building at 2nd and 1st floors. This pattern confirms the rocking effect of the soil on buildings particularly at the higher floors.

Variations of displacement ratios and story shear ratios of top floor of buildings against separation gap are shown in Figure 12 and Figure 13. Response ratios are obtained from normalization of maximum response of buildings in pounding to no-pounding case. When the separation gap is equal to or greater than the minimum separation gap required to prevent pounding, displacement and story shear ratios are equal to one because separation gap between two adjacent buildings is wide enough to allow the individual building vibrate freely. Otherwise, pounding occurs and building displacements and story shears deviate from no-pounding case.

As shown in Figure 12, although pounding affects displacements of both FB and SSSI buildings but variations of displacement ratios are not significant when separation gap ratio is relatively wide (i.e. >0.06 m). For relatively narrow separation gaps (i.e. <0.06 m),

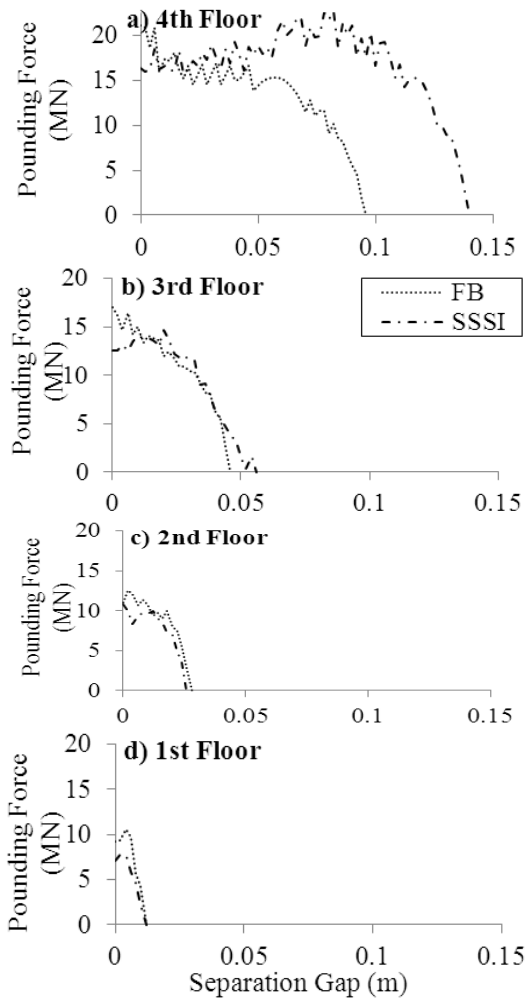

Figure 11. Pounding forces versus separation gap

displacements of top floor of 7-story FB building are decreased about 20% whereas displacements of top floor of 4-story FB building are increased about 20%. At this narrow separation gaps FB buildings show larger displacement ratios than SSSI buildings since displacements of SSSI buildings are accommodated by soil.

In case of story shear (Figure 13), pounding effect is totally against the buildings since it amplifies story shears of both buildings up to 2 times. In addition, effect of soil is significant on the story shears during pounding. Even in wide separation gaps, the story shears are amplified due to pounding. For the separation gaps ranging between 0.080 and 0.120 m, though effect of pounding on the FB buildings is negligible, but it is significantly detrimental on SSSI building where the story shears are sharply amplified. Therefore, effect of soil is negative and should be considered in the building analysis for safe design. Finally it is concluded that irrespective to the foundation condition (i.e. FB or SSSI), pounding

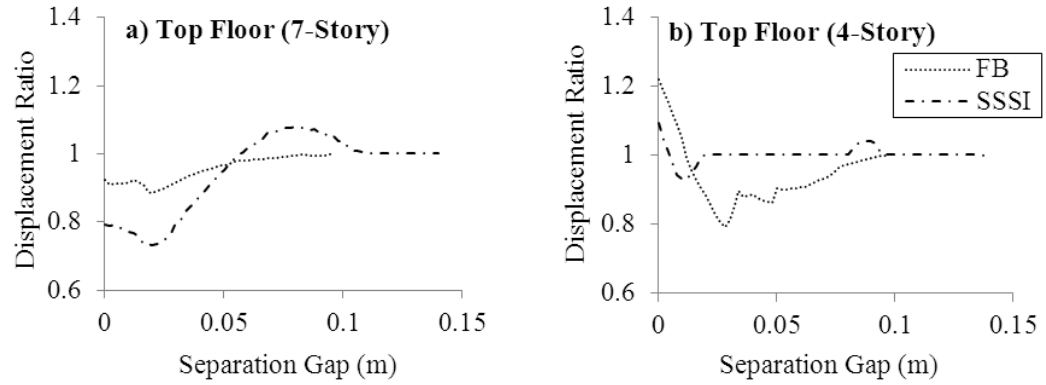

Figure 12. Displacement ratios of top floor of buildings versus separation gap

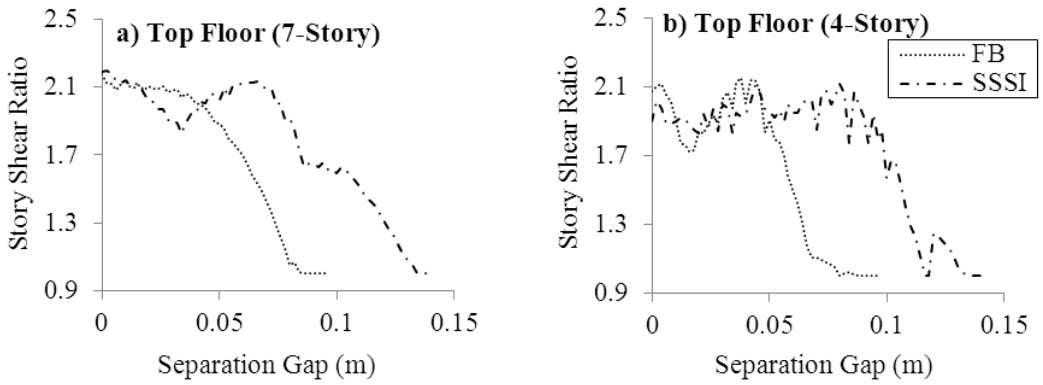

Figure 13. Story shear ratios of top floor of buildings versus separation gap

effect should be considered in the building analysis when the separation gap is less than minimum requirement to prevent pounding. Particularly, the story shears are sharply amplified even for relatively wide separation gaps, when the buildings are suspected to pound together.

4. CONCLUSIONS

A numerical model of adjacent buildings resting on a half-space was provided whilst the buildings were connected by visco-elastic contact force model. Contact force model was activated when the separation gap was closed and the buildings pounded together. Seismic responses of buildings subjected to acceleration time history of the El Centro earthquake were calculated for two foundation conditions, fixed-based (FB) and structure-soil-structure interaction (SSSI).

It was initially found that adjacent buildings resting on the soft soils were in higher risk of pounding occurrence than the same buildings resting on hard soil. Results of the analyses of adjacent buildings subjected to earthquake induced pounding showed amplification of the

seismic responses of buildings which was detrimental to the buildings. The critical condition occurred at top floor of buildings where story shears were increased dramatically. Effect of pounding was more remarkable for relatively narrow separation gaps. It was also found that soil altered building seismic responses and the buildings experienced greater seismic responses due to soil even in relatively wide separation gaps. If the adjacent buildings are suspected to pound together, pounding effects should be considered and the buildings should be modelled together with the soil.

REFERENCES

1. Rosenblueth E, Meli R. The 1985 Earthquake: causes and effects in Mexico city, *Concrete International (ACI)*, No. 5, **8**(1986) 23-36.
2. Kasai K, Maison BF. Building pounding damage during the 1989 Loma Prieta earthquake, *Engineering Structures*, No. 3, **19**(1997) 195-207.
3. EERI. 1999 Kocaeli, Turkey, *Earthquake Reconnaissance Report*, Earthquake Engineering Research Institute, California, USA, 2000.
4. Mucciarelli M, Masi A, Vona M, Gallipoli MR, Harabaglia P, Caputo R, Piscitelli P, Rizzo E, Picozzi M, Albarello D, Lizza C. Quick Survey of the Possible Causes of Damage Enhancement Observed in San Giuliano after the 2002 Molise, Italy Seismic Sequence, *Journal of Earthquake Engineering*, No. 4, **7**(2003) 599-614.
5. GRM. *2007 Niigata Chuetsu-Oki Japan Earthquake Reconnaissance Report*, Global Risk Miyamoto, California, USA, 2007.
6. GRM. *2008 Sichuan Earthquake Disaster Chronicle: Through the Eyes of the First Foreign Engineers Onsite*, Global Risk Miyamoto California, USA, 2008.
7. GRM. *2009 M6.3 L'Aquila, Italy, Earthquake Field Investigation Report*, Global Risk Miyamoto California, USA, 2009.
8. IBC. *International Building Code*, International Code Council Inc., Country Club Hills, Illinois, USA, 2009.
9. TBC. *Seismic Provisions*: Taiwan Building Code, Construction and Planning Administration Ministry of Interior, Taiwan, 1997.
10. Lin JH, Weng CC. A study on seismic pounding probability of buildings in Taipei Metropolitan area, *Journal of the Chinese Institute of Engineers*, No. 2, **25**(2002) 123-35.
11. Lin JH. Evaluation of seismic pounding risk of buildings in Taiwan, *Journal of the Chinese Institute of Engineers*, No. 5, **28**(2005) 867-72.
12. INBC. *Loading Chapter: Iranian National Building Code*, Building and Housing Research Center, Tehran, Iran, 2005.
13. Penzien J. Evaluation of building separation distance required to prevent pounding during strong earthquakes, *Earthquake Engineering and structural Dynamics*, **26**(1997) 849-58.
14. Hao H, Shen J. Estimation of relative displacement of two adjacent asymmetric structures, *Earthquake Engineering and structural Dynamics*, **30**(2001) 81-96.
15. Lin JH, Weng CC. Probability analysis of seismic pounding of adjacent buildings,

Earthquake Engineering and structural Dynamics, **30**(2001) 1539-57.
16. Garcia DL, Soong TT. Assessment of the separation necessary to prevent seismic pounding between linear structural systems, *Probabilistic Engineering Mechanics* **24**(2009.a) 210-23.
17. Garcia DL, Soong TT. Evaluation of current criteria in predicting the separation necessary to prevent seismic pounding between nonlinear hysteretic structural systems, *Engineering Structures*, **31**(2009.b) 1217-29.
18. Jeng V, Kasai K. Spectral relative motion of two structures due to seismic travel waves, *Journal of Structural Engineering*, No. 10, **122**(1996) 1128-35.
19. Hao H, Liu X. Estimation of required separations between Adjacent Structures under Spatial Ground Motions, *Journal of earthquake Engineering*, No. 2, **2**(1998) 197-215.
20. Naserkhaki S, Abdul Aziz FN, Pourmohammad H. Earthquake Induced Pounding between Adjacent Buildings Considering Soil Structure Interaction, *Earthquake Engineering and Engineering Vibration*, No. 3, **11**(2012.a) 343-58.
21. Savin E. Influence of Free Field Variability on Linear Soil-Structure Interaction (SSI) by Indirect Integral Representation, *Earthquake Engineering and structural Dynamics*, **32**(2003) 49-69.
22. Anagnostopoulos SA, Spiliopoulos KV. An Investigation of Earthquake Induced Pounding between Adjacent Buildings, *Earthquake Engineering and structural Dynamics*, **21**(1992) 289-302.
23. Maison BF, Kasai K. Dynamics of Pounding When Two Buildings Collide, *Earthquake Engineering and structural Dynamics*, **21**(1992) 771-86.
24. Naserkhaki S, Abdul Aziz FN, Pourmohammad H. Parametric study on earthquake induced pounding between adjacent buildings, *Structural Engineering and Mechanics*, No. 4, **43**(2012.b) 503-26.
25. Naserkhaki S, Daneshvar-Ghorbani S, Tayyebi-Tolloei D. Heavier adjacent building pounding due to earthquake excitation, *Asian Journal of Civil Engineering (BHRC)*, No. 2, **14**(2013) 349-67.
26. Clough RW, Penzien J. *Dynamics of Structures*, 3rd Edition, Computers and Structures, Inc., Berkeley, California, USA, 2003.
27. Naserkhaki S, Pourmohammad H. SSI and SSSI effects in seismic analysis of Twin buildings: discrete model concept, *Journal of Civil Engineering and Management*, No. 6, **18**(2012) 890-8.
28. Padron LA, Aznarez JJ, Maeso O. dynamic structure soil structure interaction between nearby piled buildings under seismic excitation by BEM-FEM model, *Soil Dynamics and Earthquake Engineering*, **29**(2009) 1084-96.
29. Komodromos P, Polycarpou PC, Papaloizou L, Phocas MC. Response of seismically isolated buildings considering poundings, *Earthquake Engineering and structural Dynamics*, **36**(2007) 1605-22.
30. Newmark NM. A Method of computation for structural dynamics, *Journal of the Engineering Mechanics Division (ASCE)*, **85**(1959) 67-94.